RM L51J24

NACA RM L51J24

NACA

RESEARCH MEMORANDUM

THE UNSYMMETRICAL LOAD AND BENDING MOMENT ON THE HORIZONTAL TAIL OF A JET-POWERED BOMBER MEASURED IN SIDESLIPPING FLIGHT

By T. V. Cooney

Langley Aeronautical Laboratory
Langley Field, Va.

NATIONAL ADVISORY COMMITTEE
FOR AERONAUTICS

WASHINGTON
January 10, 1952

NATIONAL ADVISORY COMMITTEE FOR AERONAUTICS

RESEARCH MEMORANDUM

THE UNSYMMETRICAL LOAD AND BENDING MOMENT ON THE HORIZONTAL TAIL OF A JET-POWERED BOMBER MEASURED IN SIDESLIPPING FLIGHT

By T. V. Cooney

SUMMARY

Results are presented of an analysis of unsymmetrical tail-load and bending-moment measurements made during sideslipping flight tests of a jet-powered bomber airplane having a horizontal tail with 12° of geometric dihedral.

The unsymmetrical loads and moments due to dihedral and to induction effects from the vertical tail are deduced from the measurements. A comparison of the results with estimates based on available theory was found to be favorable, suggesting that existing methods might be used to modify present arbitrary design requirements relating to unsymmetrical flight conditions.

INTRODUCTION

Since a number of current airplanes have been equipped with horizontal tails which have considerable dihedral, the subject of load and moment dissymmetry over the tail has become of interest. Although it is known that the presence of dihedral results in a rolling moment and hence in an unsymmetrical load during sideslipping flight, current strength requirements do not specifically consider either this effect or the fact that load on the vertical tail induces an unsymmetrical load on the horizontal tail. Under present requirements the unsymmetrical portion of the load on the horizontal tail is related to the load that occurs at limit load factor. As a result it would be expected that for two similar airplanes having a given directional stability the one having dihedral in the horizontal tail would not have as great a margin of safety as the airplane having a flat horizontal tail.

In the investigation of tail loads being carried out on the B-45 airplane, which has a horizontal tail with 12° of dihedral, flight data have become available for studying the effect of both dihedral and vertical-tail load on the load dissymmetry over the horizontal tail. It is the purpose of this paper to present some of the data from this investigation which bear on this point and to compare experimental results with theory.

SYMBOLS

λ	horizontal-tail taper ratio
q	dynamic pressure, pounds per square foot
β	sideslip angle, degrees
L_L	horizontal-tail load, left side, pounds
L_R	horizontal-tail load, right side, pounds
BM_L	horizontal-tail bending moment, left side, inch-pounds
BM_R	horizontal-tail bending moment, right side, inch-pounds
$L_L - L_R$	horizontal-tail load dissymmetry, pounds
$BM_L - BM_R$	horizontal-tail bending moment dissymmetry, inch-pounds
L_V	vertical-tail load, pounds
Γ	dihedral angle of horizontal tail, radians
S	horizontal-tail area, square feet
b	horizontal-tail span, inches
C_{l_β}	rate of change of rolling-moment coefficient C_l with sideslip angle β
C_{N_β}	rate of change of unsymmetrical lift coefficient C_N with sideslip angle β

With any of the above symbols, the prefix Δ represents an increment measured from the trim condition.

APPARATUS AND TESTS

Airplane and instruments.- The airplane used for this investigation is powered by four jet engines and is classed as a medium bomber. A three-view drawing of the test airplane is shown in figure 1 and pertinent geometric characteristics are given in table I. The airplane weight during the tests was approximately 60,000 pounds and the center of gravity was located at approximately 28 percent of the mean aerodynamic chord.

During the tests standard NACA recording instruments were used to measure airspeed, altitude, sideslip angle, control positions, linear accelerations, and angular velocities. Structural loads and bending moments on the horizontal and vertical tail surfaces were measured by electrical strain-gage bridges mounted on the spars near the root of each surface (see fig. 1). In order to obtain aerodynamic loads and bending moments, the inertia loads and moments, computed from the normal and transverse accelerations at the tail, were added to the structural loads and moments obtained from the strain-gage measurements. A 0.1-second time pulse was used to correlate the records of all recording instruments.

Flight tests.- The data used in the present analysis were obtained from measurements made in rudder kicks and gradual sideslips at Mach numbers from 0.40 to 0.74 at a pressure altitude of approximately 30,000 feet. In the rudder-kick maneuvers, the rudder was displaced abruptly to the left to various positions and then held constant while the sideslip was allowed to increase to a maximum value. No appreciable change in speed or altitude occurred during these maneuvers. In the sideslip maneuvers, the sideslip angle was gradually increased in nonturning flight while the airspeed was maintained constant. In these latter maneuvers nearly steady sideslipping conditions were considered to prevail at each instant since the change in sideslip angle was less than $\frac{1}{2}^{\circ}$ per second. In both types of maneuvers the airplane was in the clean condition and in trimmed steady flight at the start.

ANALYSIS AND RESULTS

Treatment of experimental data.- Neglecting effects of power, the unsymmetrical load on a horizontal tail with dihedral can be considered to be made up of two components; one due to the geometric dihedral in sideslip and the other due to induction effects from a load on the vertical tail. For purposes of analyzing the experimental data it was found convenient to write this unsymmetrical load in the form

$$\Delta\left(L_L - L_R\right) = \left[\frac{\partial\,\Delta\left(L_L - L_R\right)}{\partial\,\Delta\beta}\right]\Delta\beta + \left[\frac{\partial\,\Delta\left(L_L - L_R\right)}{\partial\,\Delta L_V}\right]\Delta L_V \qquad (1)$$

where $\Delta\left(L_L - L_R\right)$, $\Delta\beta$, and ΔL_V are incremental values measured from the conditions existing at the start of the maneuver and the bracketed terms are to be evaluated.

In order to determine the bracketed terms, the values of $\Delta\beta$, ΔL_V, and $\Delta\left(L_L - L_R\right)$ obtained from the flight records for each 1/10 second in a continuous run were substituted in equation (1). The resulting simultaneous equations involving the measured variables were then solved by a least-squares procedure for the unknown values of the bracketed coefficients $\left[\frac{\partial\,\Delta\left(L_L - L_R\right)}{\partial\,\Delta\beta}\right]$ and $\left[\frac{\partial\,\Delta\left(L_L - L_R\right)}{\partial\,\Delta L_V}\right]$.

The data obtained in 23 rudder-kick runs were analyzed in this manner to obtain the variation of the bracketed terms with dynamic pressure.

The bending-moment dissymmetry was written in the form

$$\Delta\left(BM_L - BM_R\right) = \left[\frac{\partial\,\Delta\left(BM_L - BM_R\right)}{\partial\,\Delta\beta}\right]\Delta\beta + \left[\frac{\partial\,\Delta\left(BM_L - BM_R\right)}{\partial\,\Delta L_V}\right]\Delta L_V \qquad (2)$$

and the flight data were analyzed in the manner outlined for the load dissymmetry using measured values of $\Delta\left(BM_L - BM_R\right)$, $\Delta\beta$, and ΔL_V and solving by a least-squares procedure for the values of the bracketed terms in equation (2).

The data obtained in gradual sideslip maneuvers could not be subjected to the foregoing type of analysis since in these maneuvers a definite relationship exists at each instant between the sideslip angle and the vertical-tail load. Substitution in equation (1) of the variables $\Delta\beta$, ΔL_V, and $\Delta\left(L_L - L_R\right)$ representing conditions at various times during the sideslip maneuver resulted in a set of simultaneous equations which were multiples of one another. However, when values of the bracketed coefficients obtained from the analysis of the rudder kicks were multiplied by the values of $\Delta\beta$ and ΔL_V measured in gradual sideslips, the resulting unsymmetrical loads and moments were found to represent the gradual sideslip flight measurements.

The four bracketed coefficients $\left[\frac{\partial \Delta(L_L - L_R)}{\partial \Delta\beta}\right]$, $\left[\frac{\partial \Delta(L_L - L_R)}{\partial \Delta L_V}\right]$, $\left[\frac{\partial \Delta(BM_L - BM_R)}{\partial \Delta\beta}\right]$, and $\left[\frac{\partial \Delta(BM_L - BM_R)}{\partial \Delta L_V}\right]$ of equations (1) and (2) determined in the manner outlined previously are shown in figures 2 and 3 plotted against the dynamic pressure of the maneuver.

Theoretical effect of dihedral.- An analytical study of the effect of dihedral given in reference 1 indicates that the rolling moment of an isolated tail should increase linearly with the dihedral angle and with the angle of sideslip. This rolling moment may be written in the form

$$\text{Rolling moment} = \frac{C_{l_\beta}}{\Gamma} \Gamma\beta q S b \tag{3}$$

where Γ is the geometric dihedral in radians. Since the rolling moment of this isolated tail is equal to the difference of the right and left tail root bending moments, equation (3) can be rewritten as follows:

$$\Delta(BM_L - BM_R) = \frac{C_{l_\beta}}{\Gamma} \Gamma\beta q S b \tag{4}$$

Values of $\frac{C_{l_\beta}}{\Gamma}$, as defined in equations (3) and (4), have been derived from lifting-surface theory calculations in reference 2 for wings of various aspect and taper ratios having dihedral portions extending various amounts along the span. For the B-45 tail the value of $\frac{C_{l_\beta}}{\Gamma}$ was determined to be 0.71. Introducing this value in equation (4) together with the values of S, b, and Γ from table I yielded the difference in left and right bending moments, per degree of sideslip, shown by the solid line of figure 3(a).

An expression for the unsymmetrical load which parallels that given for the unsymmetrical bending moment is:

$$\Delta(L_L - L_R) = \frac{C_{N_\beta}}{\Gamma} \Gamma\beta q S \tag{5}$$

where C_{N_β} is the unsymmetrical load coefficient of the load distribution associated with C_{l_β}.

The data and curves of reference 2 may be used to obtain load distributions and hence values of $\frac{C_{N_\beta}}{\Gamma}$ from which the difference in load on the left and right horizontal tails due to dihedral can be calculated. For the B-45 tail the theoretical value of $\frac{C_{N_\beta}}{\Gamma}$ was determined to be 2.85. With this value of $\frac{C_{N_\beta}}{\Gamma}$ the change in unsymmetrical load, per unit sideslip angle, was calculated and is the solid line plotted in figure 2(a).

Since curves showing the variation of $\frac{C_{N_\beta}}{\Gamma}$ and $\frac{C_{l_\beta}}{\Gamma}$ with aspect ratio and taper ratio may be useful in other computations of unsymmetrical loads and moments due to sideslip, they are included herein as figure 4. Figure 4 applies to unswept tails at subsonic speeds having a uniform dihedral along the span. If the dihedral portion extends only partially along the span or if the tail is swept, then the data and curves of reference 2 may be resorted to.

Theoretical effect of vertical-tail load.- Because of the proximity of the horizontal and vertical tails, a load on either surface will be accompanied by a load on the other surface due to mutual induction effects. In order to calculate the magnitude of the load induced on the horizontal tail of the B-45 by a load on the vertical tail, a simplified lifting-surface method was employed which is similar to that given in reference 3. In the present case the lift on the vertical surface and on each span of the horizontal surface was represented by a system of nine horseshoe vortices located at the 1/4 chord as indicated in figure 5. The downwash induced by the horseshoe vortices was equated to the angle of attack of the horizontal and vertical tail surfaces at nine points on the 3/4 chord. This led to a system of linear simultaneous equations which were solved for the nine unknown vortex strengths, for the conditions of unit angle of attack of the vertical tail surface and 0° angle of attack of the horizontal tail surfaces.

The results indicated that each pound of load on the vertical tail was accompanied by an up load of 0.32 pound on one-half of the horizontal tail span and a down load of 0.32 pound on the opposite half yielding an unsymmetrical load of 0.64 pound per pound of vertical-tail load. The

resulting unsymmetrical bending moment was 47 inch-pounds per pound of vertical-tail load. These quantities are given by the solid lines in figures 2(b) and 3(b), where the ordinates are the differences in the loads and bending moments between the left and right sides of the horizontal tail per pound of vertical-tail load.

For airplanes having unswept tail surfaces, reference 4 may be useful in obtaining an estimate of the magnitude of the loads and moments induced on the horizontal tail. In this reference lifting-line theory was used to obtain load distributions over an elliptical horizontal tail mounted at the base of an elliptical vertical tail for various relative sizes of the two surfaces.

DISCUSSION

In order to illustrate the reliability of the factors obtained from analysis of the flight data, a rudder kick and a gradually increasing sideslip maneuver both performed at approximately the same dynamic pressure $\left(q = 141 \text{ lb/ft}^2\right)$ were selected. For these maneuvers the measured values of $\Delta\beta$ and ΔL_V were multiplied by the four factors (represented by the filled-in points shown in figures 2 and 3) deduced from the rudder kick to obtain the two upper curves in figures 6 to 9. These component curves were added to give the solid bottom curve which was then compared with the measured dissymmetry. It appears from the comparisons shown in the bottom part of the figure that the factors determined from the experimental data obtained in the rudder-kick maneuver serve to duplicate in detail the actual time histories in both the rudder kick and the gradual sideslip.

It is seen from figures 2 and 3 that some disagreement exists between the solid theoretical curves and the experimentally determined points. The theoretical results represent the unsymmetrical lift and moment at the center line of an isolated horizontal tail in the sideslip case and at the center line of a horizontal tail in the presence of a vertical tail having negligible thickness in the vertical-tail-load case. The experimental points, on the other hand, are the results of measurements of load and bending moment at the strain-gage stations which are outboard of these positions. A better basis for comparison would be to correct the theoretical values to the strain-gage station which in the case of the horizontal tail is 21 inches out from the center line. This correction was made by decreasing the theoretical bending moments by the product of the theoretical load and the distance from the center line to the strain-gage station, since the load due to the dihedral effect is small inboard of the strain gages. The dashed-line in figure 3(a) represents the theoretical bending moment referred to the 21-inch station. In the case of

the load induced on the horizontal tail by the vertical tail a similar correction could not be made because in this case the induced effects are a maximum at the center and taper off rapidly toward the tip.

The curves of figures 6 to 9 show that the largest contribution to the unsymmetrical load and moment on the horizontal tail is due to the dihedral effect. The contribution of the vertical-tail load to this dissymmetry can either be in the same or opposite direction to the dihedral effect, depending upon how the rudder is moved during the maneuver.

The curves of figure 4 can be used to advantage to predict the effect of dihedral on the dissymmetry, and the effect of the vertical-tail load can be calculated in specific cases by application of the lifting-surface theory. As a qualitative guide, it can be said that the effect of the vertical-tail load on the dissymmetry will vary with the plan form, size, and aspect ratio of both the horizontal and vertical surfaces as well as with the position of each relative to the other. When the horizontal tail is mounted either at the base or the tip of the vertical tail the induced load is greatest. For a vertical tail which is symmetrical about the plane of the horizontal tail, the induced effects would be zero.

CONCLUDING REMARKS

The results of an analysis of the data obtained in flight tests of a jet-powered bomber airplane indicate that the unsymmetrical horizontal tail load and bending moment due to dihedral in sideslip and due to induction effects from the vertical tail can be estimated using available theory.

Because of the agreement found between the estimates and the flight results, an approach along the lines of this analysis is suggested for rationalizing the present design criterions relating to the design of horizontal tail surfaces for the unsymmetrical flight conditions.

However, before the design requirements can be placed on a completely rational basis, it remains to specify the maximum combination of sideslip angle and vertical-tail load that an airplane is capable of attaining in a given maneuver.

Langley Aeronautical Laboratory
National Advisory Committee for Aeronautics
Langley Field, Va.

REFERENCES

1. Pearson, Henry A., and Jones, Robert T.: Theoretical Stability and Control Characteristics of Wings with Various Amounts of Taper and Twist. NACA Rep. 635, 1938.

2. DeYoung, John: Theoretical Antisymmetric Span Loading for Wings of Arbitrary Plan Form at Subsonic Speeds. NACA TN 2140, 1950.

3. Diederich, Franklin W.: Charts and Tables for Use in Calculations of Downwash of Wings of Arbitrary Plan Form. NACA TN 2353, 1951.

4. Katzoff, S., and Mutterperl, William: The End-Plate Effect of a Horizontal-Tail Surface on a Vertical-Tail Surface. NACA TN 797, 1941.

TABLE I

GEOMETRIC CHARACTERISTICS OF THE AIRPLANE

Wing:	
Airfoil section at root	NACA 66_2-215
Airfoil section at tip	NACA 66_1-212
Area, sq ft	1175.2
Span, in.	1068
Chord at root, in.	225
Chord at tip, in.	93
Dihedral, deg	1
Incidence at root, deg	3
Incidence at tip, deg	1/2
Mean aerodynamic chord, in.	168
Vertical tail:	
Airfoil section at root	NACA 65_1-012
Airfoil section at tip	NACA 65-010
Area of portion extending above horizontal tail, sq ft	108
Rudder and tab area, sq ft	29
Fin offset, deg	0
Chord at attachment to horizontal tail, in.	145
Chord at tip, in.	64
Span extending above horizontal tail, in.	150
Horizontal tail:	
Airfoil section at root	NACA 65_1-012
Airfoil section at tip	NACA 65-010
Total area, sq ft	288
Elevator and tab area, sq ft	68
Span, in.	526
Chord at root, in.	123
Chord at tip, in.	36
Dihedral, deg	12
Aspect ratio	6.7
Taper ratio	0.29

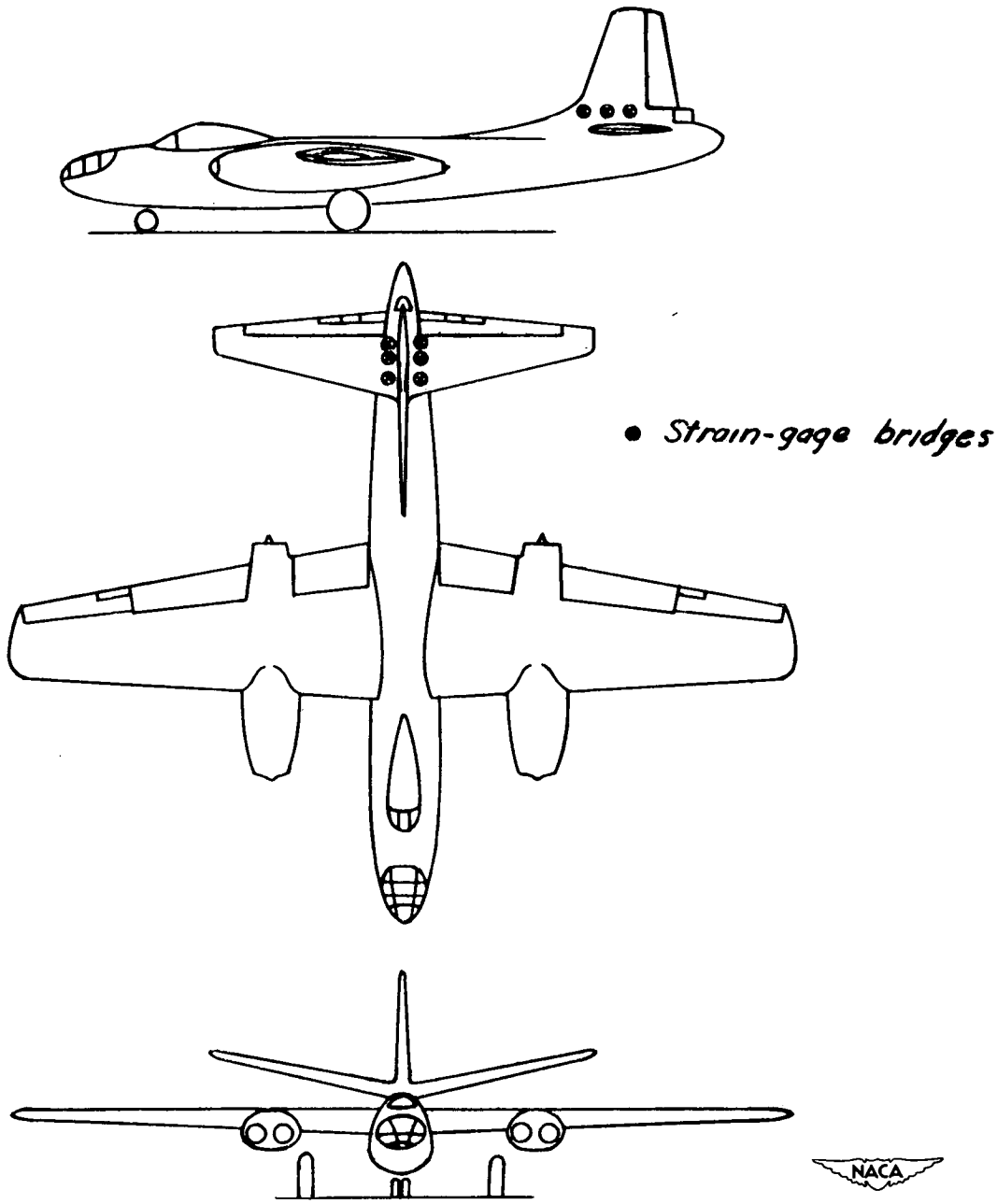

Figure 1.- Three-view drawing of test airplane showing approximate locations of strain-gage bridges on the tail surfaces.

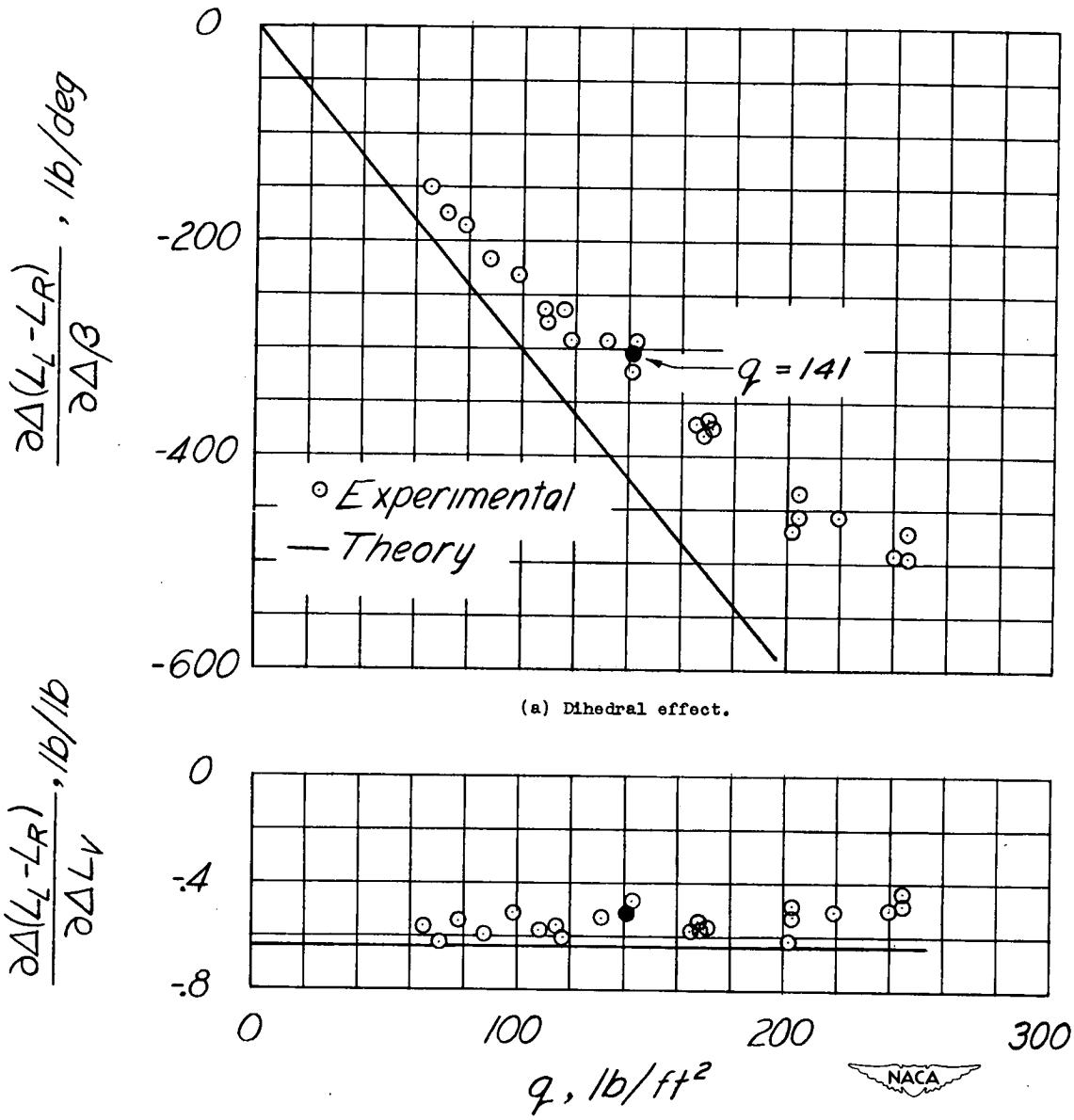

Figure 2.- Variation with dynamic pressure of coefficients for unsymmetrical load due to dihedral in sideslip and for unsymmetrical load due to induction from vertical tail. Measurements made in rudder-kick maneuvers.

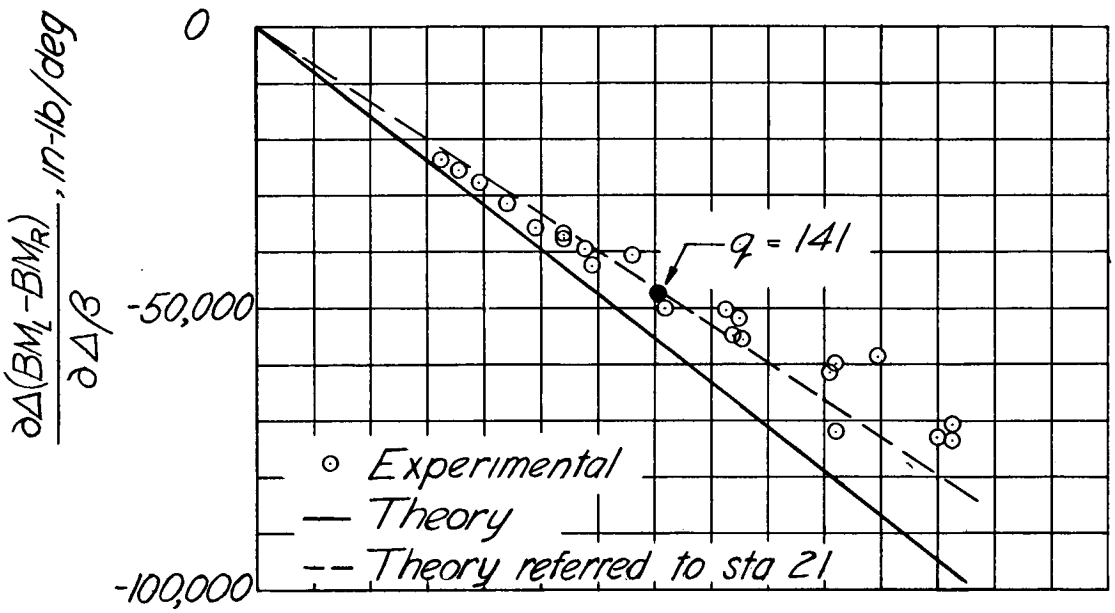

(a) Dihedral effect.

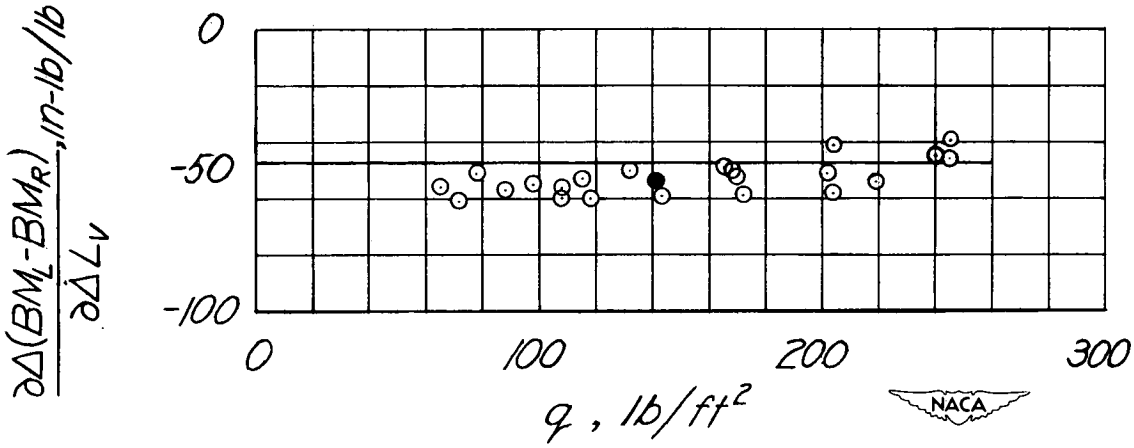

(b) Vertical-tail-load effect.

Figure 3.- Variation with dynamic pressure of coefficients for unsymmetrical bending moment due to dihedral in sideslip and for unsymmetrical bending moment due to induction from vertical tail. Measurements made in rudder-kick maneuvers.

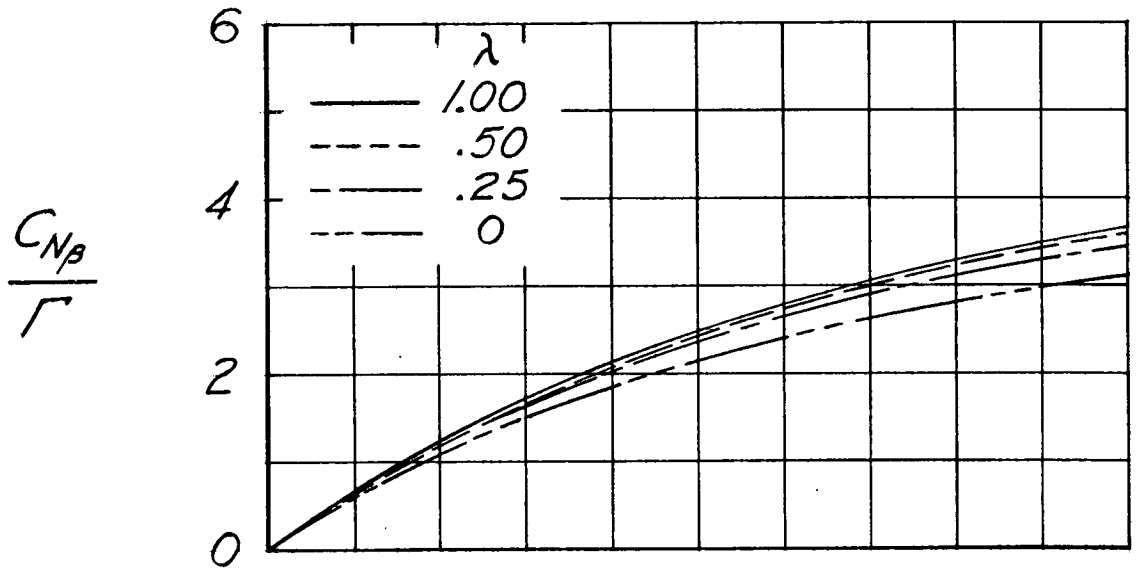

(a) Load.

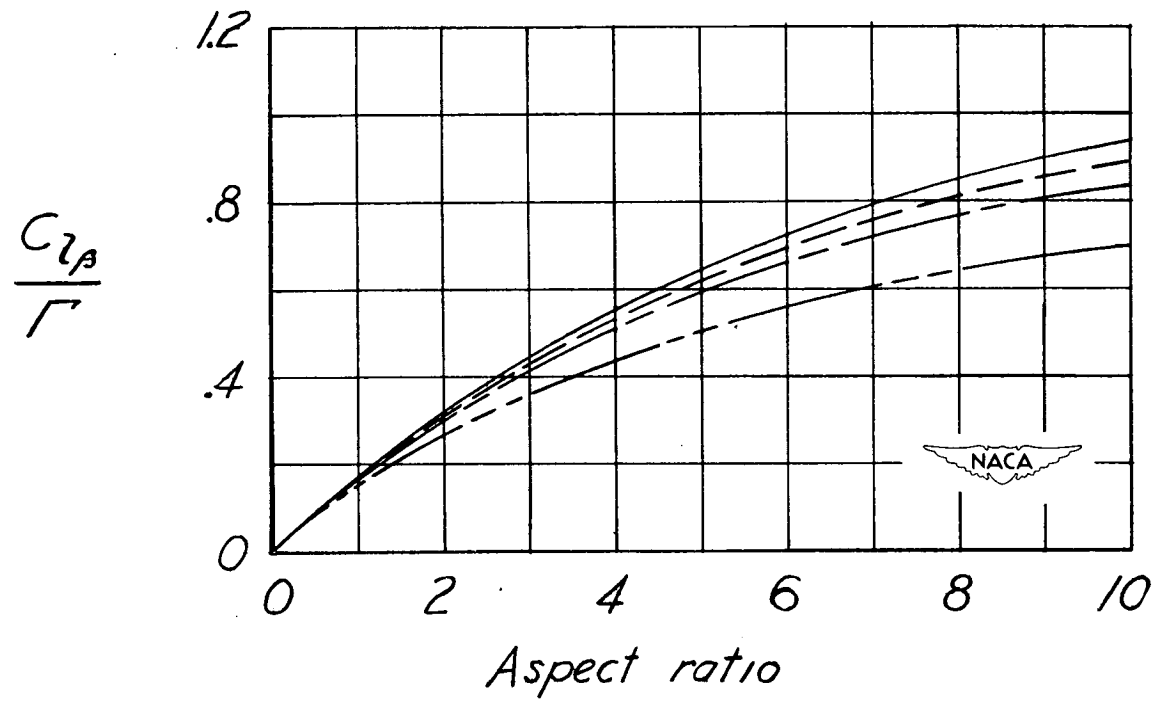

(b) Moment.

Figure 4.- Variation with aspect ratio of rolling-moment parameter and unsymmetrical-load parameter due to sideslip.

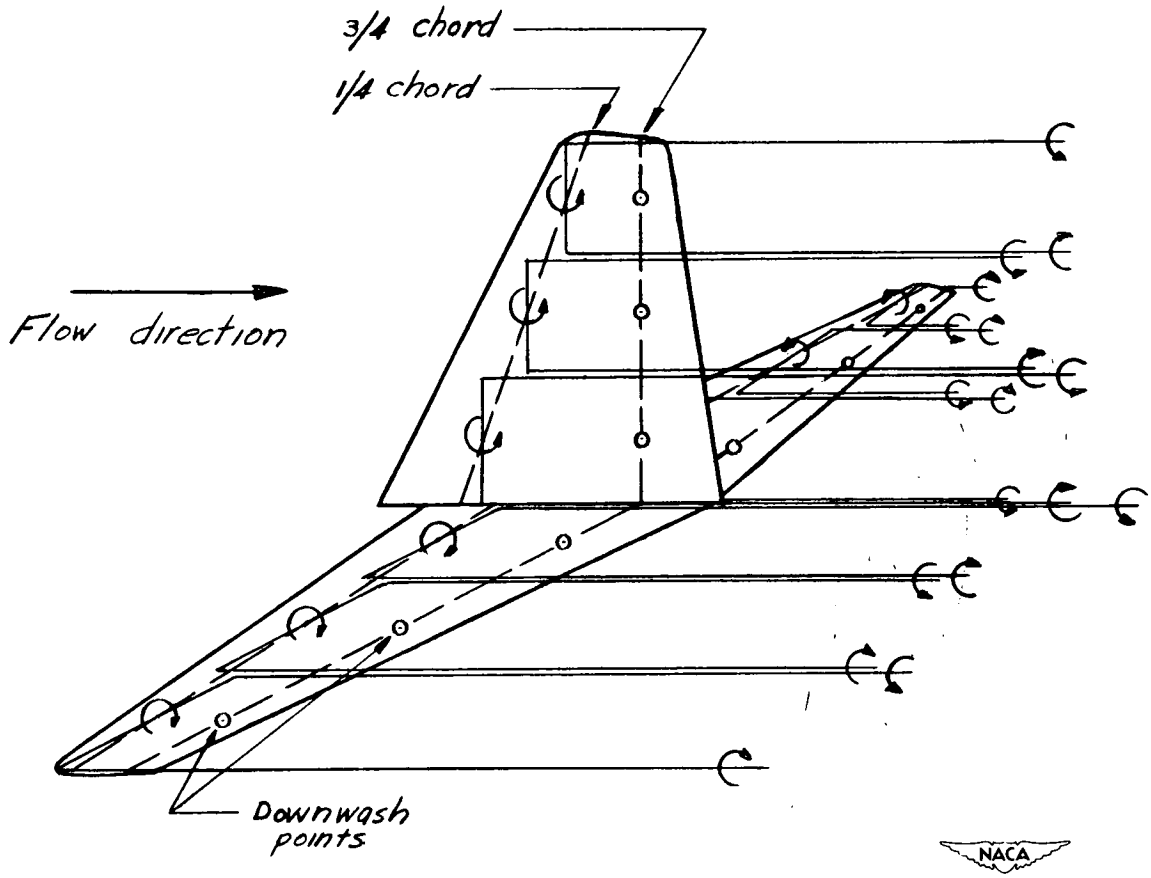

Figure 5.- Vortex system used for calculation of induced loads.

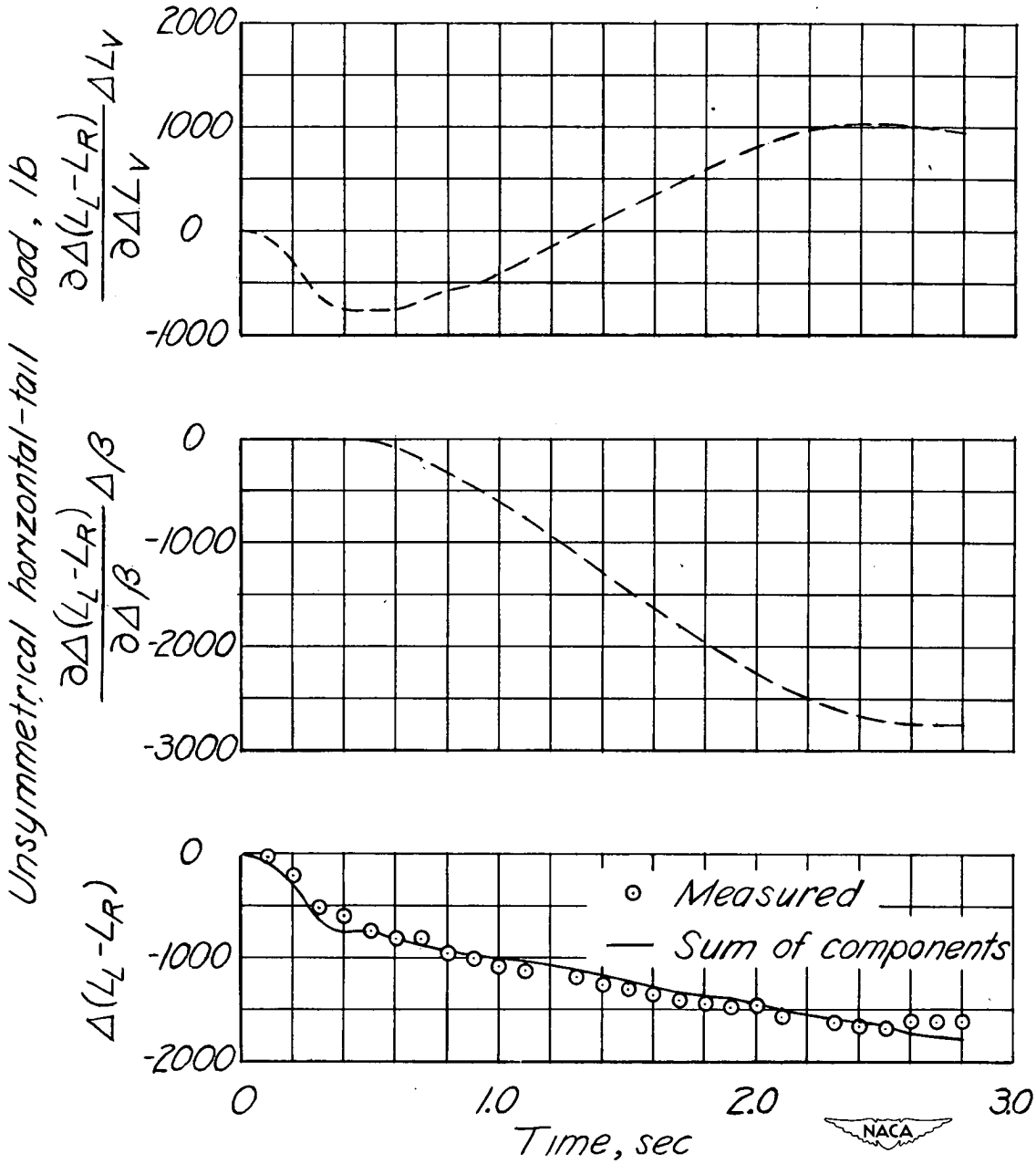

Figure 6.- Time history of rudder-kick maneuver showing comparison of measured horizontal-tail unsymmetrical load with sum of components of unsymmetrical load due to dihedral in sideslip and due to induction from vertical tail.

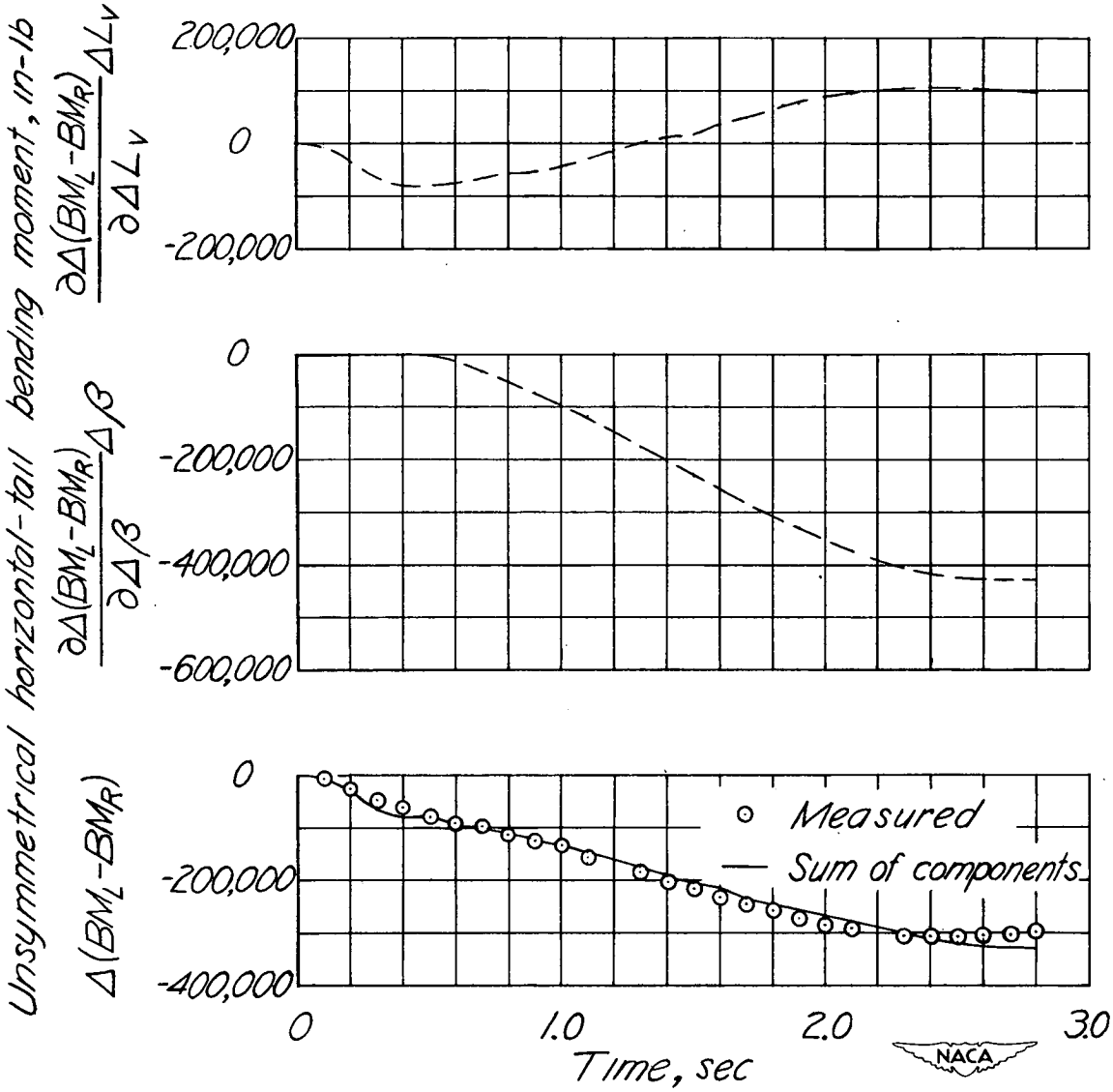

Figure 7.- Time history of rudder-kick maneuver showing comparison of measured unsymmetrical horizontal-tail bending moment with sum of components of unsymmetrical bending moment due to dihedral in sideslip and due to induction from vertical tail.

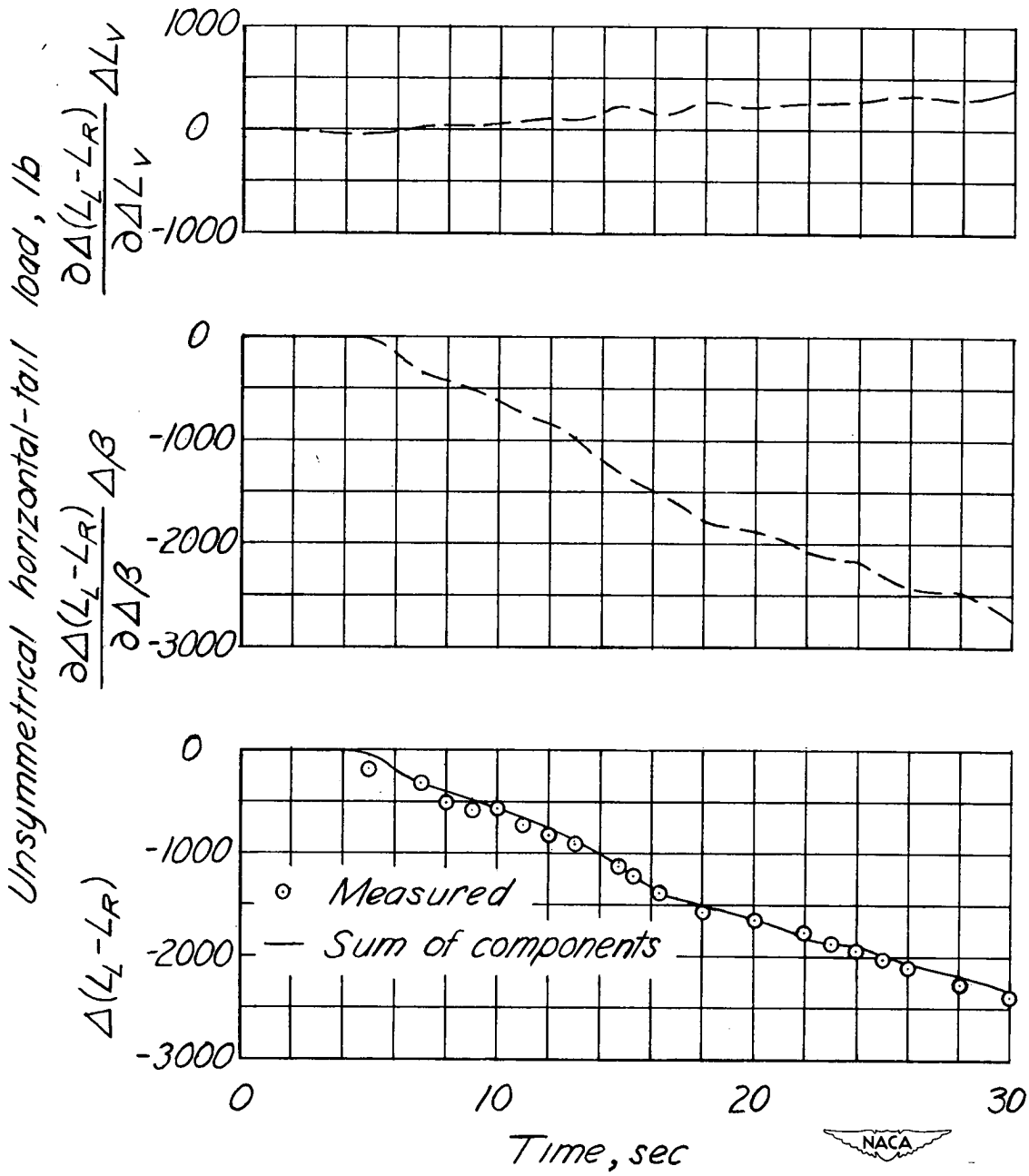

Figure 8.- Time history of gradual sideslip maneuver showing comparison of measured unsymmetrical horizontal-tail load with sum of components of unsymmetrical load due to dihedral in sideslip and due to induction from vertical tail.

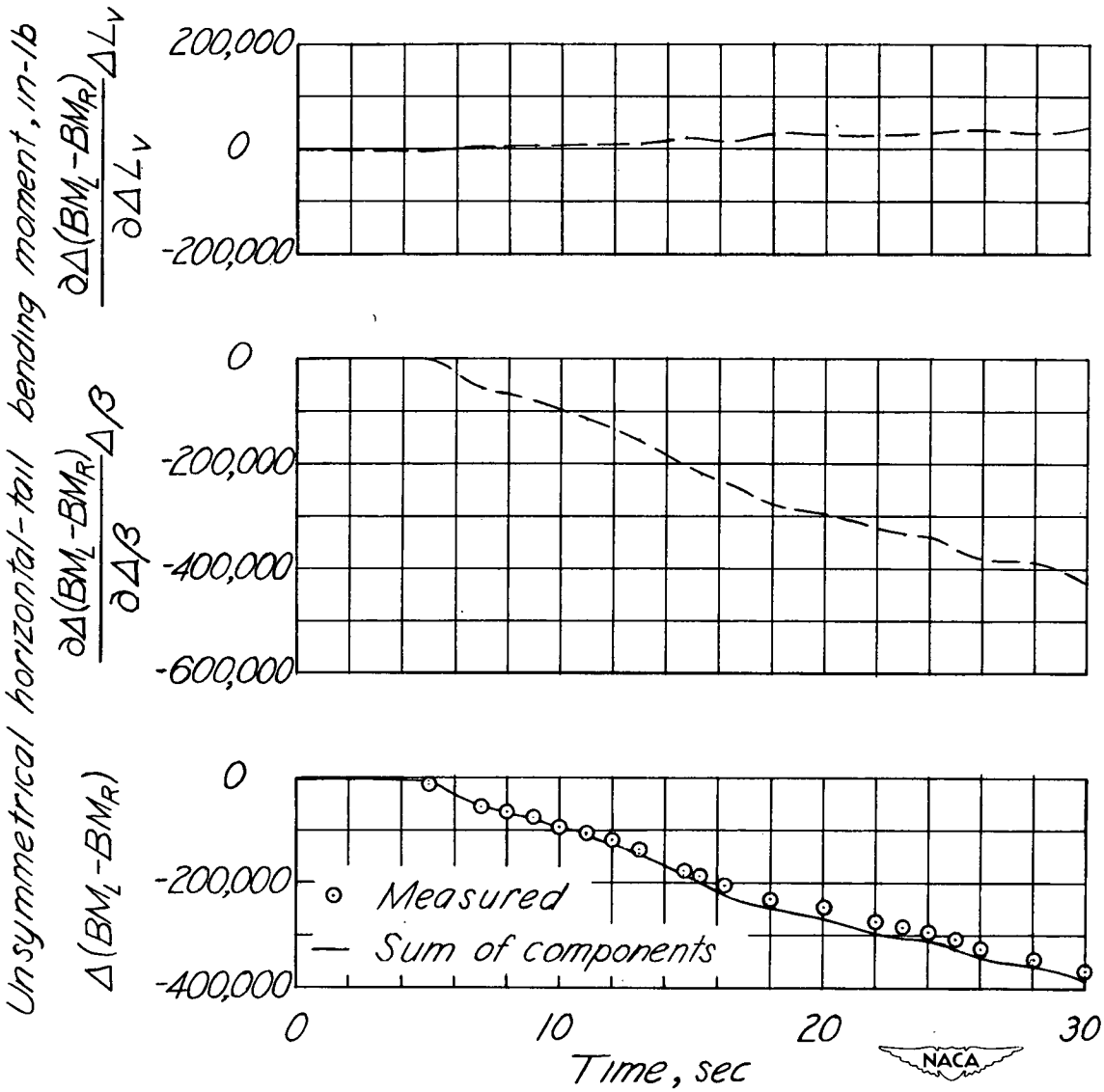

Figure 9.- Time history of gradual sideslip maneuver showing comparison of measured unsymmetrical horizontal-tail bending moment with sum of components of unsymmetrical bending moment due to dihedral in sideslip and due to induction from vertical tail.